(2)

ON THE FEASIBILITY OF A TRANSIENT DYNAMIC DESIGN ANALYSIS

by

Patrick F. Cunniff
and
Robert D. Pohland

Technical Report No. 93-1

May, 1993

Department of

MECHANICAL ENGINEERING

of

THE UNIVERSITY OF MARYLAND

(2)

ON THE FEASIBILITY OF A TRANSIENT DYNAMIC DESIGN ANALYSIS

by

Patrick F. Cunniff
and
Robert D. Pohland

Technical Report No. 93-1

May, 1993

N00014-91-J-4059

TABLE OF CONTENTS

ABSTRACT

This report examines the degree of success that may be achieved by using simple equipment-vehicle models that produce time history responses which are equivalent to the responses that would be achieved using spectral design values employed by the Dynamic Design Analysis Method. These transient models are constructed by attaching the equipment's modal oscillators to the vehicle which is composed of rigid masses and elastic springs. Two methods have been developed for constructing these transient models. Each method generates the parameters of the vehicle so as to approximate the required damaging effects, such that the transient model is excited by an idealized impulse applied to the vehicle mass to which the equipment modal oscillators are attached. The first method, called the Direct Modeling Method, is limited to equipment with at most three-degrees of freedom and the vehicle consists of a single lumped mass and spring. The Optimization Modeling Method, which is based on the simplex method for optimization, has been used successfully with a variety of vehicle models and equipment sizes.

INTRODUCTION

The Dynamic Design Analysis Method (DDAM) [1] has been used for the past 30 years as part of the Navy's efforts to shock-harden heavy shipboard equipment. This method, which has been validated several times [2], employs normal mode theory [3,4] and design shock values [5]. Current DDAM practice prescribes a modal analysis approach that utilizes these shock design values in three orthogonal directions and takes into account the type of vehicle, and equipment location, i.e., hull-mounted, deck-mounted, and shell-plate mounted. Recent papers have provided an overview on the evolution of spectral techniques in naval shock design [6]; guidance to account for structural interactive effects in choosing design shock values from shock spectra [7]; and the demonstration of a procedure [8] for establishing shock design curves for spectral analysis from accumulated field data.

Since the introduction of DDAM, different transient analysis methods have been proposed as alternative approaches to spectral analysis. One such method [9] uses a simple base mass to represent the vehicle to which the equipment is attached, and an impulsive force applied to the base mass so as to produce shock excitation. Recent papers [10, 11] examined the degree of success that may be achieved by simple equipment-vehicle models that produce time history responses whose modal maximum response values are equivalent to those of DDAM.

This report summarizes the major points made in the two papers published under the current grant [10, 11], and presents new material on the formulation of acceptable transient models.

BACKGROUND

Consider an equipment attached to the vehicle in Fig.1(a) that is subject to a shock excitation. The equipment may be replaced by a dynamically equivalent modal model composed of its normal mode oscillators as shown in Fig.1(b), where by dynamical equivalence we mean that the response of the vehicle is identical for the systems in Fig.1(a) and (b). The mass of each oscillator is called the modal effective mass and the frequency of each oscillator equals the corresponding fixed base natural frequency of the equipment. Knowing these modal characteristics, we can calculate the set of modal shock design values, N, from typical design curves such as those in Fig.2. A way of arriving at these curves can be found in reference [8]. Having the modal shock design values, the characteristic loads are applied to the equipment model in order to calculate the modal deflections and stresses. These modal quantities are added by means of the NRL sum. This is essentially the DDAM approach for estimating the maximum deflections and stresses experienced by heavy equipment.

Each design curve in Fig.2 is for a constant modal effective weight and is represented by the linear equation:

$$N=(\omega^2\frac{X}{g})f=(2\pi\frac{V_{max}}{g})f \tag{1}$$

where f is the fixed base frequency of the equipment in Hz, and $V_{max} = \omega X$ is the maximum pseudo-velocity. The maximum value of the acceleration N_{max} for the given modal effective mass is also known, so that eq.(1) is applicable up to the corner frequency f_c, where

$$f_c=(N_{max}g)/(2\pi V_{max}) \tag{2}$$

If the fixed base frequency of the equipment is greater than the corner frequency, V_{max} is reduced to V as shown in Fig.3 and the modal acceleration remains N_{max}.

In place of using design curves the following set of typical equations [5] are used herein for calculating the shock design values V_a in in/s and N_a in g's given the modal effective weight W_a in kips:

$$V_a=20\frac{(480+W_a)}{(100+W_a)} \text{ and } N_a=10.4\frac{(480+W_a)}{(20+W_a)} \tag{3}$$

DIRECT MODELING APPROACH

Two-Degree of Freedom Equipment Model

Figure 4 shows the vehicle consisting of mass M_0 and spring K_0 supporting a two-degree of freedom equipment represented by its two modal oscillators. M_1 and M_2 are the modal effective masses, K_1 and K_2 are the modal springs, and β and γ are the fixed base frequencies of the equipment, where $\beta < \gamma$. The system is excited by an impulse applied to the base mass. It is assumed that the equipment modal characteristics are known so that the DDAM inputs can be calculated from eq. (3) in the form of the pseudo-velocities $V_1=\beta X_1$ and $V_2=\gamma X_2$.

The problem centers on selecting the base mass, the vehicle frequency ϕ, where $\phi^2 = K_0/M_0$, and the magnitude of the impulse velocity V_0 so that the ensuing time history motion of the modal model produces an equivalent shock damage potential as predicted by a DDAM analysis. Thus, if we scale the modal oscillator relative displacement X_1 by β and X_2 by γ, the peak amplitudes of each time history should be equal to the shock design values βX_1 and γX_2 prescribed by the DDAM inputs.

Analysis

The frequency equation for the three-degree of freedom system in Fig.4 is

$$(\phi^2-\omega^2)(\beta^2-\omega^2)(\gamma^2-\omega^2) - \mu\beta^2\omega^2(\gamma^2-\omega^2) - \tau\gamma^2\omega^2(\beta^2-\omega^2) = 0 \qquad (4)$$

in which $\mu = M_1/M_0$ and $\tau = M_2/M_0$. A general schematic locating the roots ω_1, ω_2, and ω_3 is shown in Fig. 5. The region for the equipment fixed base frequency β, where $\omega_1 < \beta < \omega_2$, and the fixed base frequency γ, where $\omega_2 < \gamma < \omega_3$, are shown along with the vehicle frequency ϕ.

The response of the equipment modal mass M_2 relative to the base mass is:

$$-X_2/V_0 = (A/\omega_1)\sin\omega_1 t + (B/\omega_2)\sin\omega_3 t + (C/\omega_3)\sin\omega_3 t \qquad (5)$$

in which

$$A = (\omega_1^4 - \omega_1^2\beta^2)/(\omega_2^2 - \omega_1^2)(\omega_3^2 - \omega_1^2)$$

$$B = (\omega_2^4 - \omega_2^2\beta^2)/(\omega_1^2 - \omega_2^2)(\omega_3^2 - \omega_2^2)$$

$$C = (\omega_3^4 - \omega_3^2\beta^2)/(\omega_1^2 - \omega_3^2)(\omega_2^2 - \omega_3^2)$$

It can be shown that

$$|X_2/V_0|_{max} = Q/D \qquad (6)$$

in which

$$Q = (\beta^2\omega_1^2-\omega_1^4)(\omega_3^2-\omega_2^2)\omega_2\omega_3 + (\omega_2^4-\omega_2^2\beta^2)(\omega_3^2-\omega_1^2)\omega_3\omega_1 + (\omega_3^4-\omega_3^2\beta^2)(\omega_2^2-\omega_1^2)\omega_1\omega_2$$

$$D = \omega_1\omega_2\omega_3(\omega_2^2-\omega_1^2)(\omega_3^2-\omega_1^2)(\omega_3^2-\omega_2^2)$$

Likewise,

$$|X_1/V_0|_{max} = R/D \qquad (7)$$

in which $R = (\gamma^2\omega_1^2-\omega_1^4)(\omega_3^2-\omega_2^2)\omega_2\omega_3 + (\gamma^2\omega_2^2-\omega_2^4)(\omega_3^2-\omega_1^2)\omega_1\omega_3 + (\omega_3^4-\omega_3^2\gamma^2)(\omega_2^2-\omega_1^2)\omega_1\omega_2$

Equations (6) and (7) form the ratio of the shock design values as:

$$r = \beta X_1/\gamma X_2 = \beta R/\gamma Q \qquad (8)$$

Knowing the ratio r from eq.(3), the problem is to find W_0 and ϕ so that the terms on the right side of eq.(8) are satisfied. Once this is achieved, eqs. (6) and (7) may be rearranged to find the relationship for V_0 as:

$$V_0 = \beta X_1 D/\beta R \quad \text{or} \quad V_0 = \gamma X_2 D/\gamma Q \qquad (9)$$

The transient modal model is now complete. Assigning the initial velocity V_0 to the base of weight W_0 and knowing the vehicle frequency ϕ, the ensuing time history motion of βX_1 and γX_2 should produce peak values equal to the prescribed shock design values.

It is interesting to let $W_0 = \infty$ so that μ and τ are zero in eq.(4). It follows that the system frequencies are ϕ, β, and γ. Equation (8) reduces to

$$\phi = \beta\frac{(1-r)}{\left(\frac{\beta}{\gamma}-r\right)} \qquad (10)$$

Since ϕ must be positive and $\beta < \gamma$, there is a gap where eq.(10) holds, namely, $\beta/\gamma < r < 1$. It was observed that for the limited number of examples studied values of ϕ less than ϕ in eq.(10) could never yield a transient model that satisfies its DDAM design ratio r.

Finally, if we let W_0 approach zero in eq.(8), it reduces to $r = \beta/\gamma$.

Example 1

Let the modal effective weights for the two-degree of freedom equipment in Fig.4 be 26 kips and 60 kips and the corresponding fixed base frequencies equal 27 Hz and 61 Hz, respectively. The shock design values, obtained from eq.(3) are $\beta X_1 = 80.31746$ in/s and $\gamma X_2 = 67.50000$ in/s so that the ratio $r = 1.1899$. Note that this is the type of system for which a solution was unattainable when the vehicle spring K_0 was not present [10]. Figure

6 contains plots of the ratio r as a function of the base weight W_0 for fixed values of the vehicle frequency ϕ. These include $\phi = \beta$ and $\phi = 0.5\beta$, both of which provide a value W_0 by intersecting the straight line representing the ratio r; $\phi = \gamma = 2.259\beta$ which does not intersect the r-line; and $\phi = 0.254\beta$ obtained from eq.(10) which approaches the r-line asymptotically as W_0 approaches infinity. Table 1 summarizes the results for the two designs that provide viable transient models.

TABLE 1 - Example 1

DDAM βX_1 = 80.3175 in/s DDAM γX_2 = 67.5000 in/s

Design	ϕ(Hz)	W_0(kips)	V_0(in/s)	$\lvert\beta X_1\rvert_{max}$	$\lvert\gamma X_2\rvert_{max}$
1	27	79.44	67.9910	79.0696	66.1933
			69.0641	80.3175	67.2380
2	13.5	251.40	60.1793	79.9947	67.4454
			60.2280	80.0594	67.5000

The values listed in the fifth and sixth columns are the maximum absolute values of the responses of the modal masses for the initial velocity V_0. After the first trial run, V_0 was scaled so as to provide a more accurate value of the required peak values of βX_1 and γX_2. Figure 7 shows the base motion for Designs 1 and 2 from which the response spectra in Fig. 8 were obtained. Note that since the base motions are different for the two designs, the corresponding shock response spectra are also different. However, we observe that the shock design values at the fixed base natural frequencies of the equipment are identical, as indeed they should be.

THREE-DEGREE OF FREEDOM EQUIPMENT

Consider the modal model for the three-degree of freedom equipment shown in Fig.9 attached to the vehicle of mass M_0 and spring K_0. As in the case of the two-degree of freedom equipment, the base mass is excited by an impulse producing an initial velocity V_0. Knowing the equipment fixed base frequencies β, γ, and δ, where $\beta < \gamma < \delta$, and the modal effective weights, the DDAM-like shock design values are calculated and labeled βX_1, γX_2, and δX_3. The analysis of the maximum response of the relative motion of each modal oscillator is similar to the two-degree of freedom equipment except that there are now two independent ratios to satisfy from the three shock design ratios defined as follows:

$$r_1 = \beta X_1/\gamma X_2;\ r_2 = \beta X_1/\delta X_3;\ \text{and } r_3 = \gamma X_2/\delta X_3.$$

The equations for finding these ratios are summarized in Appendix A. It is emphasized that the desired vehicle parameters W_0 and ϕ must be found such that the two independent

ratios are equal to their respective DDAM values. This requires a trial and error process that is described in the following example.

Example 2

Table 2 lists the modal effective weights, the fixed base frequencies, and the shock design ratios for the three-degree of freedom modal equipment model in Fig.9.

TABLE 2 - Example 2

i	Modal Weight, W_i (kips)	Frequency, f_i (Hz)	Ratio, r_i
1	60	58	0.8406
2	26	61	0.7576
3	10	90	0.9012

A trial and error procedure is used to find the base frequency ϕ such that the plot of two of the ratios corresponding to the largest modal weights intersect their DDAM design ratio value at the same W_0. This is achieved by finding the value of W_0 at each point of intersection, say W_{01} for the r_1 plot and W_{02} for the r_2 plot. A solution is normally found rather rapidly by examining the change in sign in $\Delta W_0 = (W_{01} - W_{02})$ as ϕ is varied. For this example a value of $\phi/\beta = 0.9475$ was found after eight iterations that gave satisfactory results shown in Fig.10. Note that all three r-plots intersect their design ratios at $W_0 = 455$ kips.

Example 3

Let the overhanging 10WF25 beam support three equal lumped masses each equal to 25.88 lb-s^2/in as shown in Fig.11. Table 3 lists the modal effective weights, the fixed base frequencies and the shock design ratios.

TABLE 3 - Example 3

i	Modal Weight, W_i (kips)	Frequency, f_i (Hz)	Ratio, r_i
1	2.103	6.205	1.1868
2	27.572	17.884	0.9862
3	0.325	54.808	0.8310

Figure 12 shows the cross-over points for each ratio occurring at $W_0 = 90.25$ kips for the case where $\phi = 0.367\ \beta$. Figures 13(a-c) show the time responses of the scaled relative displacements where $V_0 = 82.1748$ in/s. The measured peaks values from these data points are compared with the DDAM shock design values as follows:

βX_1 = 93.013 in/s versus 94.435 in/s
γX_2 = 79.374 in/s versus 79.574 in/s
δX_3 = 95.754 in/s versus 95.754 in/s

The difference between the measured versus the desired values are due primarily to roundoff errors and a finite time increment of 0.001 seconds in the time history response.

OPTIMIZATION MODELING APPROACH

Background

The direct modeling approach is appropriate when the equipment has at most three degrees of freedom. This method is impractical for equipment with more than three degrees of freedom because the algebra becomes unwieldy and there are too many ratios to satisfy by the trial-and-error method. Therefore, an alternative method was investigated which could handle equipment with higher degrees of freedom.

An optimization method was chosen which minimizes the error between the time-history responses of modal oscillators and the desired DDAM values. As in the case of the Direct Modeling Approach the equipment is attached to a vehicle that is excited by an ideal impulse. The vehicle's parameters are optimized so that the absolute maximum (peak) responses of the oscillators closely match the prescribed DDAM inputs. In this approach, the number of degrees of freedom of the vehicle and equipment are not as narrowly limited. It will be shown from the examples that as the number of DOF of the vehicle increases, the number of DOF of the equipment may also grow in order to maintain acceptable error levels.

Modeling for Optimization

A. Vehicles

Six vehicles were used in the optimization scheme as shown in Figure 14. Vehicles 2, 4, 5, and 6 are grounded, whereas vehicles 1 and 3 are free-free structures. The modal frequencies and mode shapes are obtained by solving for the eigenvalues (modal frequencies) and eigenvectors (mode shapes) of the differential equation of motion, written in matrix form as follows:

$$[M^{-1}K - \omega^2 I][X] = 0 \qquad (11)$$

in which

M = an n^{th} order mass matrix
K = an n^{th} order stiffness matrix
ω = fixed base natural frequency
X = displacement vector

Since vehicles 1 and 3 are free-free systems, normal mode theory states that they will exhibit rigid-body motion in mode 1, and the first modal frequency will be identically zero. Solving for the eigenvalues and eigenvectors numerically gives rise to round-off errors. For the free-free systems, the numerical calculation of the first modal frequency is not identically zero due to the inherent errors in the code; therefore, the code employs the method of matrix deflation when using the non-grounded vehicles to correct this inconsistency.

The matrix deflation method reduces the $M^{-1}K$ matrix (dynamic matrix) from an n^{th} order to an $(n-1)^{th}$ order matrix without disrupting the eigensolution. It uses the knowledge that the mode shape of a free-free system in mode 1 is a vector of all ones. From the

orthogonality relation of normal modes, the leading matrix is then reduced to a matrix of order (n-1) (refer to Appendix B). This deflated matrix, known as the reduced dynamic matrix, contains the same modal frequencies and mode shapes for all remaining modes (i.e. all modes except mode 1) as the original dynamic matrix. By this method, the modal frequency in mode 1 is set to zero, its corresponding mode shape is given all ones, and the remaining modes and mode shapes are determined by standard numerical methods.

B. Error Functions

The optimization routine updates the parameters of the vehicle such that the absolute maximum responses of the modal oscillators to an ideal impulse most closely match the DDAM inputs. To do so, the code minimizes an appropriate error function which serves as the criteria for evaluating the responses and moving them toward the DDAM input solution. Several error functions that were used in this investigation are described below.

1. Root-mean-square error function:

$$E_{rms} = \sqrt{(Q_1 - \bar{Q}_1)^2 + (Q_2 - \bar{Q}_2)^2 + \cdots + (Q_n - \bar{Q}_n)^2} \qquad (12)$$

in which

Q_i = time-history absolute maximum response of each modal oscillator

$\bar{Q}_i$ = DDAM input

This error function is quite useful in obtaining modal responses close to the prescribed DDAM input values; however, all the errors are equally weighted. With this error function, it is possible to have large percentage errors between the time-history responses and the DDAM design values for some oscillators and very little percentage error for others. It is often desirable to weight the errors to ensure the errors are distributed more evenly.

2. Weighted rms error function:

$$E_{rms,weighted} = \sqrt{A_1(Q_1 - \bar{Q}_1)^2 + A_2(Q_2 - \bar{Q}_2)^2 + \cdots + A_n(Q_n - \bar{Q}_n)^2} \qquad (13)$$

in which

A_i = weighting factor

These two error functions are quite effective for optimizing the responses, but they have no physical meaning. New error functions which would have a more functional application were explored. Since DDAM decrees a set of modal oscillators that transmit

loads to the base support, it seems reasonable to express these forces in terms of the root mean square summation as follows:

$$F_{DDAM,rms} = g\sqrt{(M_1\bar{N}_1)^2 + (M_2\bar{N}_2)^2 + \cdots + (M_n\bar{N}_n)^2} \tag{14}$$

in which

M_i = modal masses

$\bar{N}_i$ = DDAM accelerations (g's)

g = acceleration of gravity

Similarly, normal mode theory shows that the force transmitted across the boundary from the equipment to the vehicle is identical for both the lumped equipment model and the modal oscillator model (as shown in Figure 1). Therefore, an analogous rms force equation can be written for the time-history acceleration responses of the oscillators. By comparing the two force equations, an error function of the rms force transmitted across the boundary from the equipment to the vehicle, where the gravitation constant is neglected, is formulated.

3. Rms force error function:

$$E_{force,rms} = \sqrt{M_1^2(N_1 - \bar{N}_1)^2 + M_2^2(N_2 - \bar{N}_2)^2 + \cdots + M_n^2(N_n - \bar{N}_n)^2} \tag{15}$$

in which N_i = time-history absolute maximum acceleration response of each modal oscillator

Another means of evaluating the error is by summing the individual force contributions of each oscillator. Each oscillator will render a magnitude of force

$$F_{i,act} = M_i g N_i \tag{16}$$

Relating these forces to the respective DDAM forces offers another appropriate error function of the force. Once again the gravitation constant is neglected.

4. Actual force error function:

$$E_{force,act} = M_1\left|(N_1 - \bar{N}_1)\right| + M_2\left|(N_2 - \bar{N}_2)\right| + \cdots + M_n\left|(N_n - \bar{N}_n)\right| \tag{17}$$

The error functions of eqs.(15) and (17) are both appropriate; however, the latter error function is experimentally preferable because for a given set of responses, the error from the actual force function is larger than for the rms force counterpart. Therefore, the solution is further from zero and more easily minimized.

All four error functions listed above, however, were tested to some degree before making the actual force error the function of choice. In the early stages of the optimization efforts, the rms error function [eq.(12)] was used to solve examples involving two, three, and four degrees of freedom equipment attached to vehicles 2, 3, and 4 in Figure 14. Several of these examples were then reworked using the weighted rms error function [eq.(13)]. The weighted rms error function proved favorable because it allowed for more user influence on the solutions obtained. Again, though, these error functions had no physical meaning. Therefore, vehicles 5 and 6 were tested for equipment with six or more degrees of freedom using the force error functions [eqs.(15) and (17)]. The actual force error function was more efficient for the reason listed above; consequently, the examples solved using the optimization modeling method, presented later in the text, employ the actual error function of eq.(17).

Simplex Method

The minimization routine chosen for the optimization modeling method is the downhill simplex method by Nelder and Mead [12]. This multi-dimensional minimization routine was selected because it is logically quite simple and easy to implement, and is one of the few multi-dimensional minimization methods that requires only function evaluations and not derivatives. For our purposes, the computational burden is small and the additional efficiency associated with the gradient techniques is not necessary or desired. Reference [13] provides the computer code that has been developed for the simplex method.

A simplex is a geometrical figure consisting, in N dimensions, of N+1 vertices and all their interconnecting points, polygonal faces, etc.. In other words, if the vehicle has three parameters (design variables) to minimize, the simplex will have four vertices. Each vertex will have three coordinates, corresponding to the three design variables, specifying its position in the design space. Visually, the simplex will be a tetrahedron in 3-space as shown in Figure 15.

To begin the minimization, a starting simplex must be chosen. Let $\mathbf{P}_0$ be the initial guess vertex. A favorable choice for the other vertices is the following:

$$\boldsymbol{P}_i = \boldsymbol{P}_0 + \alpha \boldsymbol{e}_i \tag{18}$$

in which

$\mathbf{e}_i$ = directional vectors

α = arbitrary length scale constant

The length scale constant multiplied by the directional vector e_i serves to expand the i^{th} vertex in only one coordinate direction. For example, let

$$P_0 = \begin{bmatrix} x_1 \\ y_1 \\ z_1 \end{bmatrix}$$

The other vertices, obtained using eq.(18), are the following:

$$P_1 = \begin{bmatrix} x_1 + \alpha x_1 \\ y_1 \\ z_1 \end{bmatrix}; \quad P_2 = \begin{bmatrix} x_1 \\ y_1 + \alpha y_1 \\ z_1 \end{bmatrix}; \quad P_3 = \begin{bmatrix} x_1 \\ y_1 \\ z_1 + \alpha z_1 \end{bmatrix} \tag{19}$$

These four vertices and all their interconnecting points make up the starting simplex. It should be noted that α can have a different value for each vertex of eq.(19). Also note that the vertices of the starting simplex can be entered in randomly (without using eq.(18)) as in Figure 15. However, the downhill simplex method is most efficient when there is a certain measure of geometric symmetry. In the examples solved by the optimization method, a length scale constant of $\alpha=2$ was found to be advantageous.

Using the initial simplex, the method moves the simplex "downhill" towards a solution by evaluating the error function at each of the vertices and moving the highest error vertex to a lower error position. There are four possible movements of the simplex for each iteration:

(1) move the vertex with the largest error through the opposite face of the simplex to a point of lower error (reflection);
(2) when the reflection offers a lower error, the simplex will look to expand itself in that direction so as to take larger steps;
(3) if the simplex reaches a "valley floor", it contracts itself along the transverse direction (away from the highest error vertex) in order to move down the valley;
(4) if the simplex encounters an "eye of the needle", it contracts itself in all directions, pulling itself around the vertex of lowest error.

In effect, the simplex moves through the design space by evaluating and comparing the errors at each of its vertices. It then modifies itself according to the conditions above until all the vertices of the simplex meet a desired convergence criteria. The convergence criteria built into the downhill simplex method requires that the decrease in the error function in the terminating step be fractionally smaller than some tolerance. At this point the simplex is said to surround a local minimum. A tolerance of $1x10^{-9}$ was suitable for the examples solved by this method.

Several modifications were needed to use this minimization method. To begin with, the design variables used in the optimization are mass and frequency. The existing simplex method would search for a solution for both positive and negative values of mass and frequency. Since negative mass and frequency have no physical meaning, the first revision to the simplex subroutine was made to ensure that the mass variables never became

negative. It was not necessary to constrain the frequency variables because the eigenproblem works with the square of the frequency [eq.(11)] which is always positive. The second constraint on the design variables restricted the mass variables from becoming zero. Zero mass is impossible to handle in the eigenproblem because the system overflows when trying to invert a mass matrix with a zero element in the diagonal. In the event that a mass variable becomes zero, the variable is set to unity within the simplex subroutine so as not to affect the geometry of the simplex in any significant way.

Optimization Scheme

The optimization routine minimizes on the responses from the time-histories of the modal oscillators. The eigenproblem is solved and the system's response to an ideal impulse [3] is given by the following formula:

$$y_i = I_0 \sum_a \frac{X_{ia} X_{0a}}{\omega_a \sum_k m_k X_{ka}^2} \sin \omega_a t \tag{20}$$

in which

m_i = mass m_i of the system
y_i = displacement of mass m_i
X_{ia} = mode shape for mass m_i in mode a
ω_a = system natural frequency in mode a
I_0 = ideal impulse applied to mass M_0

The displacement of mass m_i relative to the base mass M_0, scaled by λ_i, is the following:

$$\lambda_i (y_i - y_0) = \lambda_i I_0 \sum_a \frac{(X_{ia} - X_{0a}) X_{0a}}{\omega_a \sum_k m_k X_{ka}^2} \sin \omega_a t \tag{21}$$

in which

λ_i = fixed base natural frequency of mass m_i

These pseudo-velocities are comparable to the DDAM inputs V_a in eq.(3). Similarly the absolute acceleration of mass m_i due to an impulse applied at mass M_0 is the following:

$$\ddot{y}_i = -I_0 \sum_a \frac{X_{ia} X_{0a} \omega_a}{\sum_k m_k X_{ka}^2} \sin \omega_a t \tag{22}$$

These accelerations, expressed in g's, can be compared to the DDAM inputs N_a in eq.(3). Consequently, both the velocity and acceleration response equations could be used to compare the velocity or acceleration responses to their respective DDAM inputs. However, it is possible for one of the modal frequencies to be zero as in the case of a free-free system.

A zero frequency will blow up the velocity eq.(21) but not the acceleration eq.(22). For this reason, the optimization routine minimizes on the acceleration responses of the oscillators rather than the velocity responses.

Every iteration in the minimization subroutine requires updating and solving the eigenproblem and then examining the time-history records to find the peak responses. This can be extremely tedious and time consuming if a good starting solution is not known. To find a good starting solution, we examine the ratios of the maximum acceleration responses, i.e.,

$$R_{ij} = \left(\frac{\ddot{y}_i}{\ddot{y}_j}\right)_{\max,\max} = \frac{\sum_a \frac{|X_{ia} X_{0a} \omega_a|}{\sum_k m_k X_{ka}^2}}{\sum_a \frac{|X_{ja} X_{0a} \omega_a|}{\sum_k m_k X_{ka}^2}} \tag{23}$$

Notice that for n mass responses, there are (n-1) independent ratios of these responses. For convenience, choose the (n-1) independent ratios to be all with respect to mass 1. We can now use the following rms error function to get some idea as to where a solution lies.

$$E_{rms} = \sqrt{\sum_{k=2}^{n} \left(R_{1k} - \bar{R}_{1k}\right)^2} \tag{24}$$

in which

R_{1k} = *ratio of the acceleration responses of mass* 1 *to mass* k

$\bar{R}_{1k}$ = *respective DDAM acceleration ratio*

By introducing the maximum response ratios error function, we can eliminate the lengthy time-history process. Furthermore, minimization of the error function in eq.(24) gives fairly accurate results when there is a small number of modal oscillators. The results from this minimization are then used as starting values in the time-history minimization of eq.(17).

General Procedure:

Starting with a given set of modal oscillators and vehicle, the first step in the optimization method is to minimize the error function in eq.(24). Once an acceptable solution is found, the vehicle parameters of the solution are used as the P_0 vertex of the starting simplex in the time-history minimization. Finding an acceptable solution, though, can be quite tedious because in many examples, there are an infinite number of local

minima in the design space. By starting the simplex at different locations in the design space, the downhill simplex method converges to the various local minima. Therefore, finding an acceptable solution requires scanning the design space by means of the guess vector P_0 to find the best of the local minima. More details are found in Appendix C.

The second phase in the optimization modeling approach is the minimization of the time-history responses. Using the solution from the absolute sum ratios minimization, an appropriate time increment is calculated (refer to Appendix B), an initial kick-off velocity is chosen arbitrarily, and acceleration records for each oscillator are created. From these records, the peak responses are found. The kick-off velocity is then scaled (refer to Appendix B) so that the acceleration responses are comparable to the DDAM accelerations. Using the actual force error function [eq.(17)], the minimization routine converges on a "best" solution and the percentage errors between the time history acceleration peak responses and the DDAM acceleration inputs are calculated for each mode.

Example 4

To show the usefulness of the optimization modeling approach, the results of Example 3 were reproduced using the optimization routine. In this example, vehicle 2 of Figure 14 was used with the same set of modal oscillators as in Example 3. Several solutions were found using the optimization method; but, we were mainly interested in the solution discussed in Example 3. The optimized solution occurred at W_0 = 90.76 kips and ϕ = 0.366 β, with a kick-off velocity V_0 = 82.3642 in/s. In this problem, the kick-off velocity V_0 was scaled so that there would be zero percentage error between the transient velocity and the DDAM velocity for the third modal oscillator, as in Example 3. Table 4 lists the measured peak acceleration responses scaled by g/ω_i, the percentage errors between the transient pseudo-velocities of the optimization modeling method (OMM) and the DDAM inputs, and the percentage errors between the transient pseudo-velocities from the direct modeling method (DMM) and the DDAM inputs.

Table 4 - Pseudo-Velocity Responses in (in/s) for Example 4

Modal Mass	Transient Pseudo-Velocity	% Error for OMM	% Error for DMM
1	93.2758	1.23	1.51
2	79.5383	0.45	0.25
3	95.7538	0.00	0.00

It is evident that the optimization modeling approach verifies and slightly improves the solution of the direct modeling method.

Example 5

An equipment represented by six modal oscillators was attached to each of the six vehicles in Figure 14, to show how the percentage errors between the transient accelerations and the DDAM accelerations are distributed according to the choice of vehicle. Since the OMM optimizes the vehicle's parameters to acquire the best responses, we anticipated that the vehicle with the most parameters would offer the best modal responses. The modal weights and fixed-base frequencies for the six degree-of-freedom equipment are listed in Table 5.

Table 5 - Example 5

i	1	2	3	4	5	6
Modal Weight (kips)	100	80	60	26	10	6
Frequency (Hz)	20	25	58	61	75	90

Following the general procedure above, the modal oscillator responses of each vehicle were optimized. Table 5A is a tabulation of the optimized time-history peak acceleration responses in g's of each modal oscillator and the respective DDAM inputs for all vehicles.

Table 5A - Acceleration Responses in g's for Example 5

Vehicle	Mass 1	Mass 2	Mass 3	Mass 4	Mass 5	Mass 6
1	22.8192	32.2972	70.1544	100.5522	100.7881	116.5813
2	17.6455	27.3462	58.0961	86.1893	121.2948	119.3071
3	18.7691	25.1460	69.2955	79.8938	99.5137	127.0906
4	18.6140	25.3998	64.5434	79.8035	104.3233	138.1553
5	18.9529	25.9094	64.2436	80.6730	103.0229	136.7243
6	18.8122	24.9171	63.7317	79.5598	108.3465	136.3057
DDAM Accelerations	18.8778	25.3151	63.7126	79.7321	108.7397	134.3063

As expected, the transient accelerations of the oscillators more closely match the DDAM accelerations as the number of parameters of the vehicle increased. Table 5B lists the largest percentage error associated with the modal oscillator responses and the oscillator number for which it occurred.

Table 5B - Example 5

Vehicle	Largest %	Modal Mass with Largest
1	27.58	1
2	11.55	5
3	8.76	3
4	4.06	5
5	5.26	5
6	1.57	2

The largest percentage errors significantly decreased as the number of vehicle parameters increased. Therefore, for systems involving large degrees-of-freedom equipment, vehicle six is the best choice for the optimization method. It is interesting to observe that there is little difference in the results for vehicles 4 and 5, both of which have four design parameters.

Example 6

In many real systems, the modal effective masses of the equipment do not decrease in descending order, as in example 5. For example, the overhanging beam system of Example 3 has more modal effective mass in mode two than in mode one. Example 6 examines whether or not the optimization method can handle large degree-of-freedom equipment examples where the second modal oscillator has more mass than the first. For the reason listed above, vehicle 6 was used in the example. Table 6 lists the modal effective weights and fixed-base frequencies of the equipment. Appendix C describes the steps used to find the parameters of the vehicle.

Table 6 - Example 6

i	1	2	3	4	5	6
Modal Weight (kips)	80	100	60	26	10	6
Frequency (Hz)	20	25	58	61	75	90

The optimized transient accelerations of the oscillators, the respective DDAM accelerations, and the percentage errors between the two accelerations are tabulated in Table 6A.

Table 6A - Acceleration Responses in g's for Example 6

Modal Mass	Transient Acceleration	DDAM Acceleration	% Error
1	20.0651	20.2521	0.92
2	23.4074	23.5973	0.54
3	63.6255	63.7126	0.14
4	79.5716	79.7321	0.20
5	109.6985	108.7397	0.88
6	134.1451	134.3063	0.12

The percentage errors associated with each modal oscillator are all less than one percent. Therefore, it appears that problems of this nature impose no problems in the optimization method.

Example 7

Example 7 serves to illustrate the range over which the optimization method is effective. A nine degree-of-freedom equipment is optimized using vehicle 6. The modal effective weights and fixed-base frequencies of the modal oscillators are listed in Table 7.

Table 7 - Example 7

i	1	2	3	4	5	6	7	8	9
Modal Weight (kips)	100	90	75	60	45	26	15	10	6
Frequency (Hz)	20	25	40	58	61	70	75	90	95

Table 7A lists the parameters of the vehicle and the value of the step change in velocity of the base point. Table 7B is a listing of the optimized transient accelerations in $_b$'s of the nine modal oscillators, the respective DDAM accelerations, and the percentage errors.

Table 7A - Vehicle Parameters for Example 7

W_g(kips)	f_g(Hz)	W_o(kips)	f_o(Hz)	W_b(kips)	f_b(Hz)	V_o(in/s)
1914.60	95.09	230.84	59.26	317.43	37.50	275.44

TABLE 7B - Acceleration Responses in g's for Example 7

Modal Mass	Transient Acceleration	DDAM Acceleration	% Error
1	18.9115	18.8778	0.18
2	24.5534	24.4110	0.58
3	41.3025	41.2894	0.03
4	65.5762	63.7126	2.93
5	71.8709	71.8861	0.02
6	94.5727	91.4959	3.36
7	104.4270	105.0733	0.62
8	129.5284	130.4877	0.74
9	140.3157	141.7678	1.02

The largest percentage error was 3.36 percent which is relatively low. Figure 16 is a plot of a sample of the time-history response of modal mass 6. We can now suggest that if we optimize equipment with degrees of freedom greater than nine without increasing the number of vehicle parameters, the overall errors would grow with the size of equipment.

SUMMARY AND CONCLUSIONS

Two approaches were taken in developing transient modal models that replicate the damaging potential prescribed by DDAM-like inputs: the Direct Modeling Method and the Optimization Modeling Method. The Direct Modeling Method has been limited to two- and three-degree of freedom equipment because the algebra becomes prohibitive as the system grows in size. The vehicle in each case is represented by a lumped mass and a ground linear spring that is excited by an impulse applied to the mass. Experience gained in using DMM shows that the two-degree of freedom equipment provides an infinite number of acceptable transient models while the three-degree of freedom equipment normally provides only one, and possibly a second, transient model. The transient models developed in Examples 1-3 reproduced, with negligible error, the equivalent DDAM shock damage in the time history response of each oscillator.

The Optimization Modeling Method was developed to overcome the algebraic difficulties with DMM when the equipment exceeds three-degrees of freedom. The method uses the Simplex Method for optimizing the parameters that make up the vehicle, where the vehicle is selected based on the number of degrees of freedom of the equipment.

Example 4 examined the same problem as posed in Example 3, in which the equipment was composed of three-degrees of freedom and the vehicle was composed of a mass and an anchored spring. The OMM provided results that compared quite favorably with the results found in Example 3.

Examples 5 examined six different vehicles varying in complexity from a single mass (vehicle 1) to three masses and three springs (vehicle 6). Each of the six vehicles supported an equipment represented by six modal oscillators. The results clearly demonstrate that as the number of parameters of the vehicle increase, the errors produced by the transient models decrease significantly. The largest modal response error for vehicle 1 was 27.58% while the corresponding error in the case of vehicle 6 dropped to 1.57%.

In the case of Example 6, the modal mass in mode-two was chosen larger than the modal mass assigned to the mode-one mass. No unusual problems were noted in developing the transient model since the error in reproducing the DDAM shock value in each mode was less than one percent.

It was decided to examine the level of errors for a nine-degree of freedom equipment attached to the vehicle with six parameters. The results were very encouraging in that the largest modal error was less than 3.37 percent as shown in Example 7.

ACKNOWLEDGEMENTS

This study is part of a project supported by the Office of Naval Research. The content of this report does not necessarily reflect the position of policy of the government.

George J. O'Hara, a former member of the faculty in the Mechanical Engineering Department, is recognized for the major contributions he made in the development of the material contained in this report. Mr. O'Hara retired from the University in August 1992.

REFERENCES

1. Belsheim, R.O., and G.J. O'Hara, "Shock Design of Shipboard Equipment, Part I, Dynamic-Design Analysis Method," NRL Report 5545, Sept. 1960. A version also published as NAVSHIPS 250-423-30, May 1961.
2. O'Hara, G.J., "Shock Hardness Assessment of Submarine Equipment; Part V; Survival of Equipment Designed by DDAM", NRL Memorandum Report No. 3942, (U) Confidential Report, Unclassified Title, March, 1979.
3. O'Hara, G.J. and P.F. Cunniff, "Elements of Normal Mode Theory", NRL Report 5917, June 21, 1963.
4. Cunniff, P.F. and G.J. O'Hara, "Normal Mode Theory for Three-Dimensional Motion", NRL Report 6170, Jan. 5, 1965.
5. O'Hara, G.J. and R.O. Belsheim, "Interim Design Values for Shock Design of Shipboard Equipment", NRL Memorandum Report No. 1396, Feb., 1963.
6. Remmers, G., "Maurice Biot 50th Anniversary Lecture: The Evolution of Spectral Techniques in Navy Shock Design," Shock and Vibration Bulletin, Part I, 59-70, 1983.
7. O'Hara, G.J. and P.F. Cunniff, "The Shock Spectrum Dip Effect", Jr. of Sound Vibration, Vol. 103, No. 3, 311-321, Dec., 1985.
8. Cunniff, P.F. and G.J. O'Hara, "A Procedure of Generating Shock Design Values", Jr. of Sound and Vibration, Vol. 134, No. 1, 155-164, Oct. 1989.
9. A series of private communications among NAVSEA, TRC/UERD, and the University of Maryland on a proposed transient design analysis method, Spring 1990.
10. O'Hara, G.J., and P.F. Cunniff, "Time History Analysis of Systems as an Alternative to a DDAM-Type Analysis," Proceedings of the 62nd Shock & Vibration Symposium, Oct. 1991, pp. 462-472.
11. O'Hara, G.J., and Cunniff, P.F., "Time History Analysis of Systems as an Alternative to a DDAM-Type Analysis," Proceedings of the 63rd Shock and Vibration Symposium, Oct. 1992, pp. 462-472.
12. Neldor, J.A., and Mead, R., Computer Journal, Vol. 7, 1965, p. 308.
13. Press, W.H., et al, Numerical Recipes in Fortrans: The Art of Scientific Computing, Cambridge University Press, Cambridge (England): New York, 1989, pp. 289-293.

APPENDIX A
EQUATIONS FOR THE DIRECT MODELLING APPROACH

The following summarizes the equations for finding the maximum relative displacements of each of the three modal oscillators in Fig. 9:

$$\left|\frac{x_1}{v_o}\right|_{max} = \frac{n1 + n2 + n3 + n4}{d}$$

in which

$$n1 = \omega_1 (\gamma^2 - \omega_1^2)(\delta^2 - \omega_1^2)(\omega_3^2 - \omega_2^2)(\omega_4^2 - \omega_2^2)(\omega_4^2 - \omega_3^2)$$
$$n2 = \omega_2 (\gamma^2 - \omega_2^2)(\delta^2 - \omega_2^2)(\omega_3^2 - \omega_1^2)(\omega_4^2 - \omega_1^2)(\omega_4^2 - \omega_3^2)$$
$$n3 = \omega_3 (\omega_3^2 - \gamma^2)(\delta^2 - \omega_3^2)(\omega_2^2 - \omega_1^2)(\omega_4^2 - \omega_1^2)(\omega_4^2 - \omega_2^2)$$
$$n4 = \omega_4 (\omega_4^2 - \gamma^2)(\omega_4^2 - \delta^2)(\omega_2^2 - \omega_1^2)(\omega_3^2 - \omega_1^2)(\omega_3^2 - \omega_2^2)$$
$$d = (\omega_2^2 - \omega_1^2)(\omega_3^2 - \omega_1^2)(\omega_4^2 - \omega_1^2)(\omega_3^2 - \omega_2^2)(\omega_4^2 - \omega_2^2)(\omega_4^2 - \omega_3^2)$$

$$\left|\frac{x_2}{v_o}\right|_{max} = \frac{n5 + n6 + n7 + n8}{d}$$

in which

$$n5 = \omega_1 (\beta^2 - \omega_1^2)(\delta^2 - \omega_1^2)(\omega_3^2 - \omega_2^2)(\omega_4^2 - \omega_2^2)(\omega_4^2 - \omega_3^2)$$
$$n6 = \omega_2 (\omega_2^2 - \beta^2)(\delta^2 - \omega_2^2)(\omega_3^2 - \omega_1^2)(\omega_4^2 - \omega_1^2)(\omega_4^2 - \omega_3^2)$$
$$n7 = \omega_3 (\omega_3^2 - \beta^2)(\delta^2 - \omega_3^2)(\omega_2^2 - \omega_1^2)(\omega_4^2 - \omega_1^2)(\omega_4^2 - \omega_2^2)$$
$$n8 = \omega_4 (\omega_4^2 - \beta^2)(\omega_4^2 - \delta^2)(\omega_2^2 - \omega_1^2)(\omega_3^2 - \omega_1^2)(\omega_3^2 - \omega_2^2)$$

$$\left|\frac{x_3}{v_o}\right|_{max} = \frac{n9 + n10 + + n11 + n12}{d}$$

in which

$$n9 = \omega_1 (\beta^2 - \omega_1^2)(\gamma^2 - \omega_1^2)(\omega_3^2 - \omega_2^2)(\omega_4^2 - \omega_2^2)(\omega_4^2 - \omega_3^2)$$
$$n10 = \omega_2 (\omega_2^2 - \beta^2)(\gamma^2 - \omega_2^2)(\omega_3^2 - \omega_1^2)(\omega_4^2 - \omega_1^2)(\omega_4^2 - \omega_3^2)$$
$$n11 = \omega_3 (\omega_3^2 - \beta^2)(\omega_3^2 - \gamma^2)(\omega_2^2 - \omega_1^2)(\omega_4^2 - \omega_1^2)(\omega_4^2 - \omega_2^2)$$
$$n12 = \omega_4 (\omega_4^2 - \beta^2)(\omega_4^2 - \gamma^2)(\omega_2^2 - \omega_1^2)(\omega_3^2 - \omega_1^2)(\omega_3^2 - \omega_2^2)$$

APPENDIX B
Special Equations for the Optimization Modeling Approach

Matrix Deflation Method

Consider the eigenvalue/eigenvector problem

$$M^{-1}KX = \lambda X$$

in which $M^{-1}K$ is called the dynamic matrix D. By the othogonality of normal modes, we know that

$$\sum_j m_j X_{ja} X_{jb} = 0$$

$$m_1 X_{1a} X_{1b} + m_2 X_{2a} X_{2b} + \cdots + m_n X_{na} X_{nb} = 0$$

$$X_{1a} X_{1b} = -\frac{m_2 X_{2a} X_{2b}}{m_1} - \frac{m_3 X_{3a} X_{3b}}{m_1} - \cdots - \frac{m_n X_{na} X_{nb}}{m_1}$$

Using the fact that for a free-free system, the mode shape for mode 1 is a vector of all ones such that

$$X_{11} = X_{21} = \cdots = X_{n1} = 1$$

and letting b=1, we have the following relation:

$$X_{1a} = -\frac{m_2}{m_1} X_{2a} - \frac{m_3}{m_1} X_{3a} - \cdots - \frac{m_n}{m_1} X_{na} \qquad (*)$$

Using the above relation, we can write X in terms of a transformation matrix P such that X = PX, or

$$\begin{bmatrix} X_{11} & X_{12} & X_{13} & \cdots & X_{1n} \\ X_{21} & X_{22} & X_{23} & \cdots & X_{2n} \\ X_{31} & X_{32} & X_{33} & \cdots & X_{3n} \\ \vdots & \vdots & \vdots & \ddots & \vdots \\ X_{n1} & X_{n2} & X_{n3} & \cdots & X_{nn} \end{bmatrix} = \begin{bmatrix} 0 & -\frac{m_2}{m_1} & -\frac{m_3}{m_1} & \cdots & -\frac{m_n}{m_1} \\ 0 & 1 & 0 & \cdots & 0 \\ 0 & 0 & 1 & \cdots & 0 \\ \vdots & \vdots & \vdots & \ddots & \vdots \\ 0 & 0 & 0 & \cdots & 1 \end{bmatrix} \begin{bmatrix} X_{11} & X_{12} & X_{13} & \cdots & X_{1n} \\ X_{21} & X_{22} & X_{23} & \cdots & X_{2n} \\ X_{31} & X_{32} & X_{33} & \cdots & X_{3n} \\ \vdots & \vdots & \vdots & \ddots & \vdots \\ X_{n1} & X_{n2} & X_{n3} & \cdots & X_{nn} \end{bmatrix}$$

Now we rewrite the eigenvalue/eigenvector problem as

$$DPX = \lambda X$$

Multiplying the dynamic matrix D by the matrix P produces the following:

$$\begin{bmatrix} D_{11} & D_{12} & D_{13} & \cdots & D_{1n} \\ D_{21} & D_{22} & D_{23} & \cdots & D_{2n} \\ D_{31} & D_{32} & D_{33} & \cdots & D_{3n} \\ \vdots & \vdots & \vdots & \ddots & \vdots \\ D_{n1} & D_{n2} & D_{n3} & \cdots & D_{nn} \end{bmatrix} \begin{bmatrix} 0 & -\frac{m_2}{m_1} & -\frac{m_3}{m_1} & \cdots & -\frac{m_n}{m_1} \\ 0 & 1 & 0 & \cdots & 0 \\ 0 & 0 & 1 & \cdots & 0 \\ \vdots & \vdots & \vdots & \ddots & \vdots \\ 0 & 0 & 0 & \cdots & 1 \end{bmatrix} = \begin{bmatrix} 0 & R_{12} & R_{13} & \cdots & R_{1n} \\ 0 & R_{22} & R_{23} & \cdots & R_{2n} \\ 0 & R_{32} & R_{33} & \cdots & R_{3n} \\ \vdots & \vdots & \vdots & \ddots & \vdots \\ 0 & R_{n2} & R_{n3} & \cdots & R_{nn} \end{bmatrix}$$

From this matrix we get the reduced matrix R.

$$[R]_{(n-1 \times n-1)} = \begin{bmatrix} R_{22} & R_{23} & \cdots & R_{2n} \\ R_{32} & R_{33} & \cdots & R_{3n} \\ \vdots & \vdots & \ddots & \vdots \\ R_{n2} & R_{n3} & \cdots & R_{nn} \end{bmatrix}$$

The reduced matrix R is known as the dynamic matrix of the reduced eigenproblem

$$RX = \lambda X$$

The natural frequencies and mode shapes of this eigenproblem are the same as the natural frequencies and mode shapes of the original eigenproblem for all modes except mode 1. Using back substitution with eq.(*), we can solve for X_{1n}.

Optimizing Kick-off Velocity

Arbitrarily choose a guess kick-off velocity V_0'. Since the acceleration equation [eq.(22)] is linear, the kick-off velocity simply scales the acceleration. The problem thus revolves around finding a multiplier s, where $V_0 = sV_0'$, that minimizes the error. Again we shall consider an rms error function:

$$E^2 = (\bar{N}_1 - sN_1)^2 + (\bar{N}_2 - sN_2)^2 + \cdots + (\bar{N}_n - sN_n)^2$$

Minimizing on s we have

$$2E\frac{dE}{ds} = 2(\bar{N}_1 - sN_1)(-N_1) + 2(\bar{N}_2 - sN_2)(-N_2) + \cdots + 2(\bar{N}_n - sN_n)(-N_n) = 0$$

Solving for s we find that

$$s = \frac{\sum_j N_j \bar{N}_j}{\sum_j N_j^2}$$

and the appropriate kick-off velocity is

$$V_0 = sV_0'$$

Choosing an Appropriate Time Increment

We wish to keep the largest angular displacement

$$\theta_{max} = \omega_{a,max} t \leq 36^o$$

Choosing a time interval of t = 0 → 1 seconds with N increments, we can write

$$2\pi f_{a,max} \Delta T = 36^o \left(\frac{\pi}{180^o} \right)$$

or

$$\Delta T = \frac{1}{10 f_{a,max}}$$

APPENDIX C
Finding a Solution for the First Phase of the Optimization Modeling Method

The first phase of the optimization modeling method is the minimization of the absolute-sum acceleration ratios as expressed by eq.(24). Since most of the examples tested had more than one local minimum, many starting vectors $\mathbf{P}_0$ were used in the minimization process in hopes of finding the best of the local minima. Vehicles 1, 2, 3, and 4 have four or less parameters so that there are at most two mass or frequency design variables. These vehicles can be optimized with a small number of trials by arbitrarily choosing initial guess vectors $\mathbf{P}_0$. For these vehicles, each initial guess vector has at most four permutations (vehicle 4) if the mass and frequency variables are required to remain in one of the two mass and frequency slots, respectively. Choosing several guess vectors and running the minimization program for each guess vector, and all their permutations, generally locates a "good" solution without excessive number of trials. However, with vehicle 6, any guess vector can be rearranged into the 36 possible permutations (again only allowing mass variables in the mass slots and frequency variables, frequency slots). Examining all 36 permutations of various guess vectors can become quite tedious. Generally speaking, though, a good solution can be found by examining only one guess vector and its permutations (refer to Example 6 below).

Example 6

Example 6 uses vehicle 6 in the minimization. As a first choice, an initial guess vector and length scale constant

$$P_0 = \begin{bmatrix} M_x \\ f_x \\ M_0 \\ f_0 \\ M_b \\ f_b \end{bmatrix} = \begin{bmatrix} 500 \\ 25 \\ 1500 \\ 50 \\ 3000 \\ 75 \end{bmatrix} \quad ; \qquad \alpha = 2$$

was used. In this case, the mass variables of Figure 14 (M_x,M_0,M_b) correspond to (500,1500,3000) and the frequency variables (f_x,f_0,f_b) correspond to (25,50,75). For ease in understanding, let the mass variables be (a,b,c) and frequency variables be (x,y,z). Using the initial guess vector above, we know that there are 36 possible ways of rearranging this vector if we require that a, b, and c only be interchanged with one another and that x, y, and z only be interchanged with one another. Table C1 lists these 36 possible combinations in terms of (a,b,c) and (x,y,z).

Table C1 - A 6-Parameter Guess Vector has 36 Permutations

a x b y c z	a x b z c y	a y b x c z	a y b z c y	a z b x c y	a z b y c x
a x c y b z	a x c z b y	a y b x c z	a y c z b x	a z c x b y	a z c y b x
b x a y c z	b x a z c y	b y a x c z	b y a z c x	b z a x c y	b z a y c x
b x c y a z	b x c z a y	b y c x a z	b y c z a x	b z c x a y	b z c y a x
c x a y b z	c x a z b y	c y a x b z	c y a z b x	c z a x b y	c z a y b x
c x b y a z	c x b z a y	c y b x a z	c y b z a x	c z b x a y	c z b y a x

All 36 combinations were used as starting vectors in the optimization routine. The best of these solutions was found to be when the guess vector P_0 was in the following form:

$$P_0 = \begin{bmatrix} c \\ y \\ a \\ z \\ b \\ x \end{bmatrix} = \begin{bmatrix} 3000 \\ 50 \\ 500 \\ 75 \\ 1500 \\ 25 \end{bmatrix}$$

The optimized vehicle parameters for the first phase of the optimization method are listed in Table B1 where the modal mass has been replaced by the modal weight in kips.

Table B1 - Vehicle Parameters for Example 6 using Eq.(24); V_o=75.76 in/s

W_x (kips)	f_x (Hz)	W_0 (kips)	f_0 (Hz)	W_b (kips)	f_b (Hz)
372.20	50.67	268.27	83.29	342.36	38.69

The root-mean-square error in eq.(24) associated with these parameters is E = 3.44×10^{-7}. These parameters were now used as the starting vector in the second phase of the optimization routine, namely the time-history minimization. The time-history minimization resulted in new vehicle parameters which are listed in Table B2.

Table B2 - Vehicle Parameters for Example 6 using Eq.(17)

W_x (kips)	f_x (Hz)	W_0 (kips)	f_0 (Hz)	W_b (kips)	f_b (Hz)
373.53	50.48	274.50	83.63	374.52	39.37

The transmitted force error in eq.(17) associated with these parameters is E = 123.29 lb/g. It is evident from Tables B1 and B2 that there is only slight changes in the vehicle parameters when optimizing on the time-histories; hence, the solution to the absolute-sum ratios minimization did in fact offer a good starting solution.

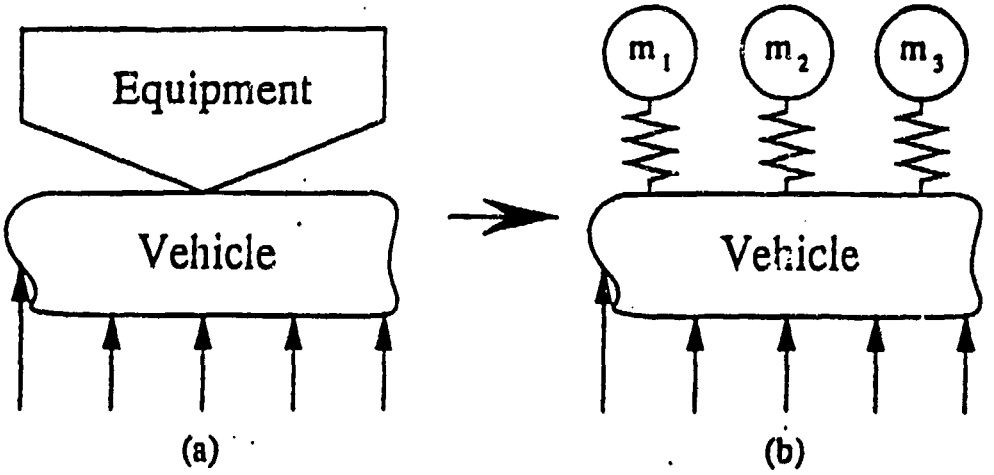

Fig. 1 - Equipment modeled by its modal oscillators.

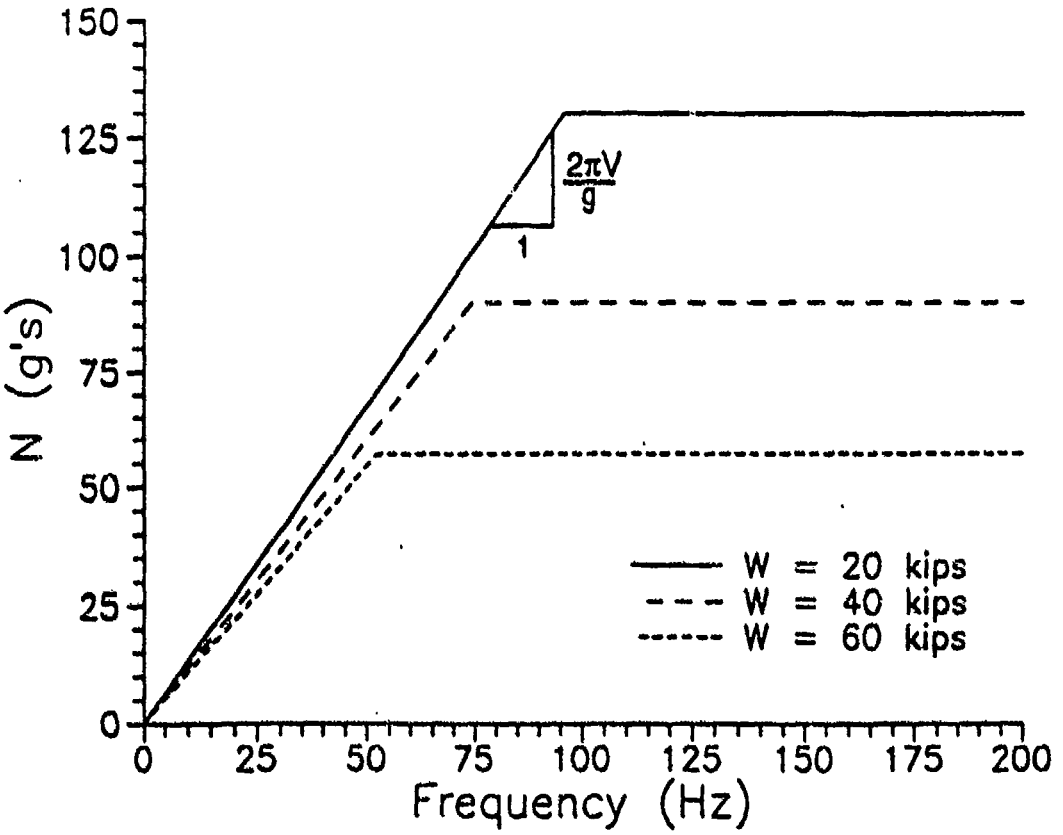

Fig. 2 - Typical shock design curves for different modal weights as a function of the fixed base frequencies.

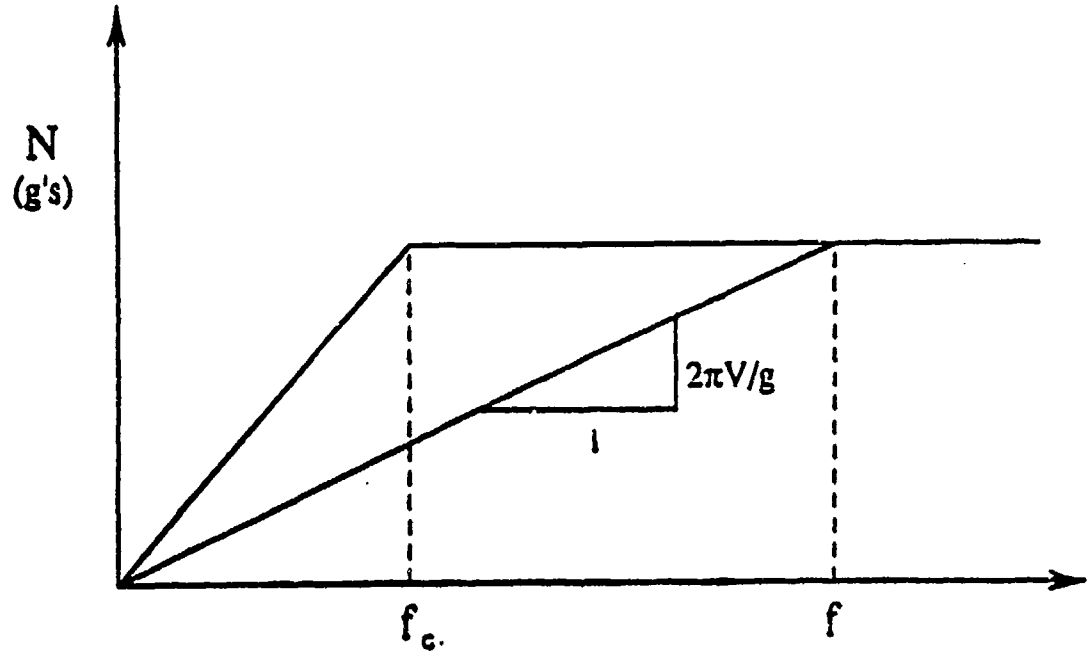

Fig. 3 - Example where the fixed base frequency is greater than the corner frequency.

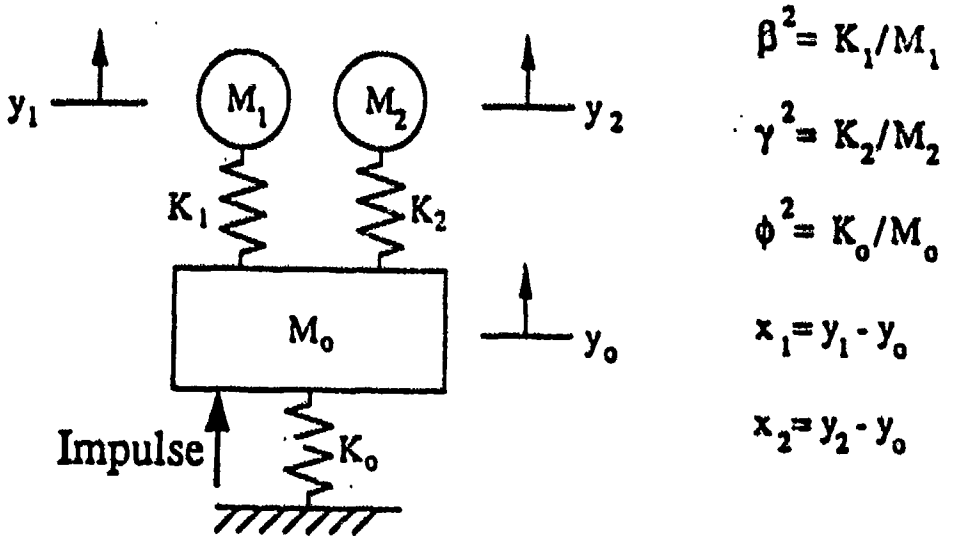

Fig. 4 - Two-degree of freedom equipment attached to the vehicle M_0, K_0.

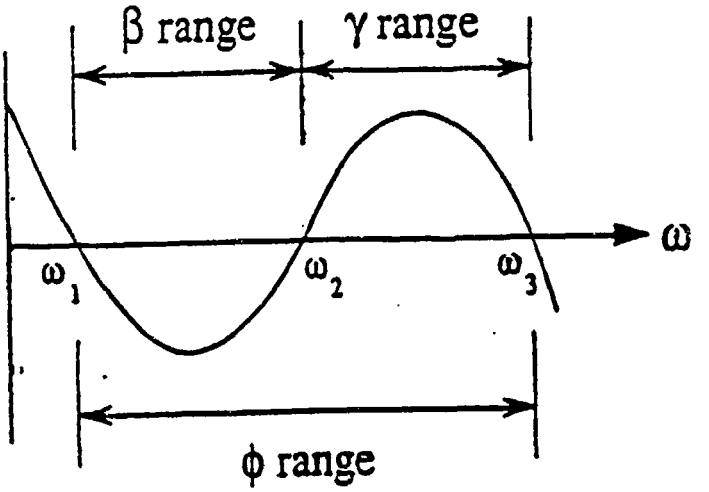

Fig. 5 - Range of the system frequencies, equipment fixed base frequencies, and the vehicle frequency.

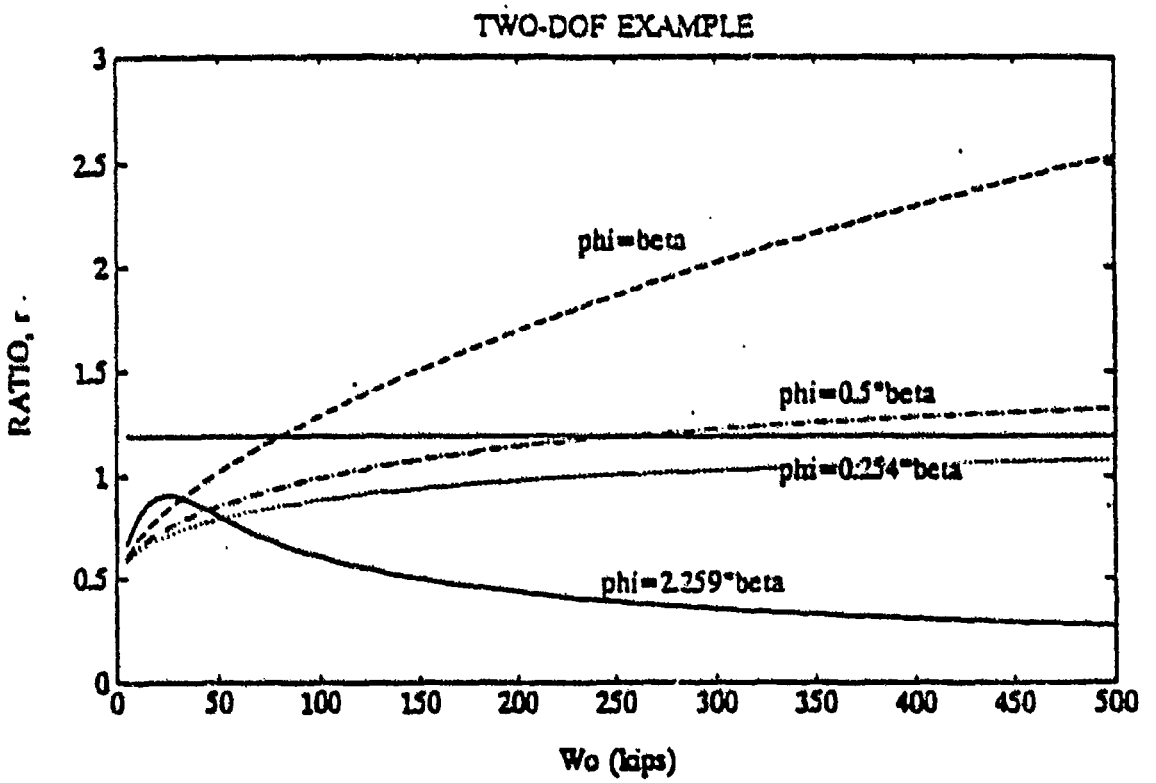

Fig. 6 - Shock design ratio as a function of the vehicle weight for fixed values of the vehicle frequency ϕ.

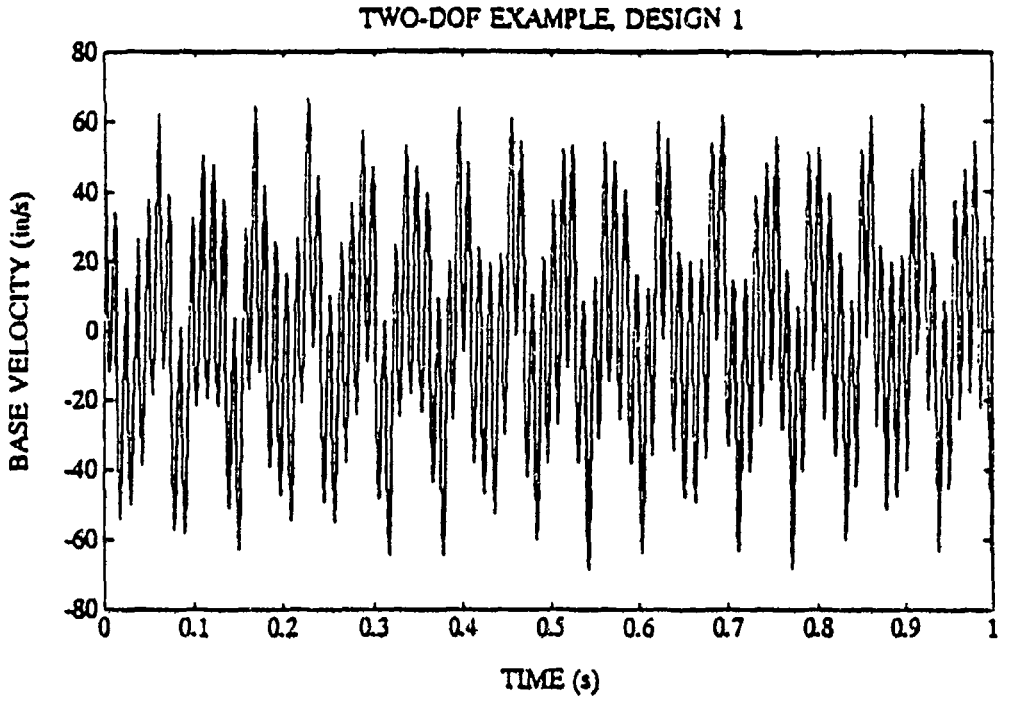

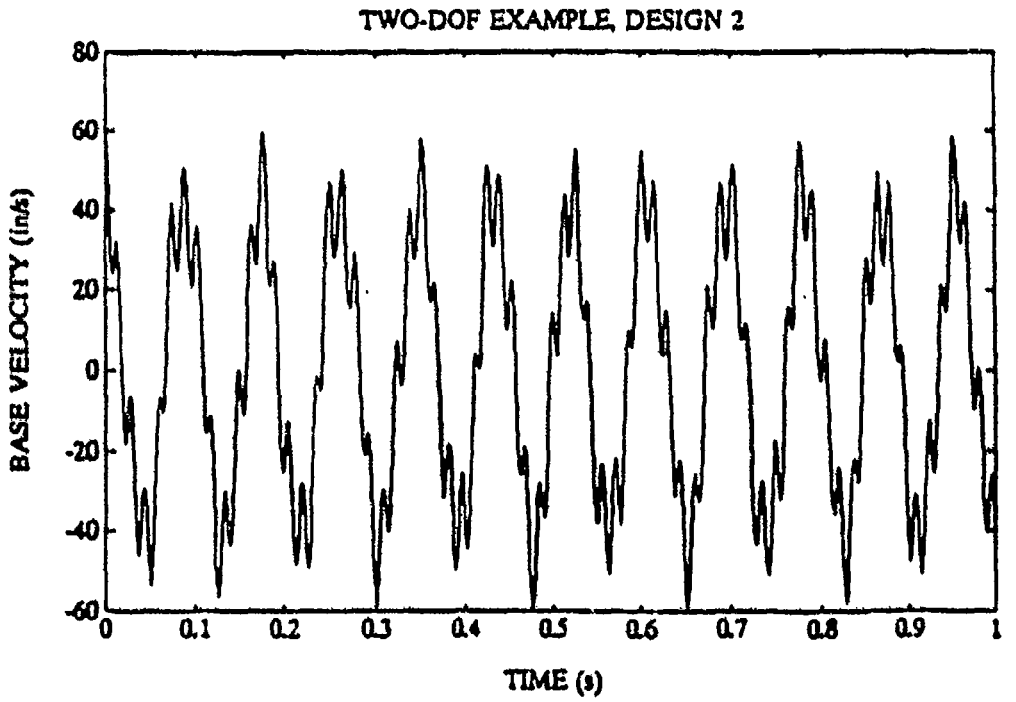

Fig. 7 - Time history motions, base velocity, Design 1 and Design 2, Example 1.

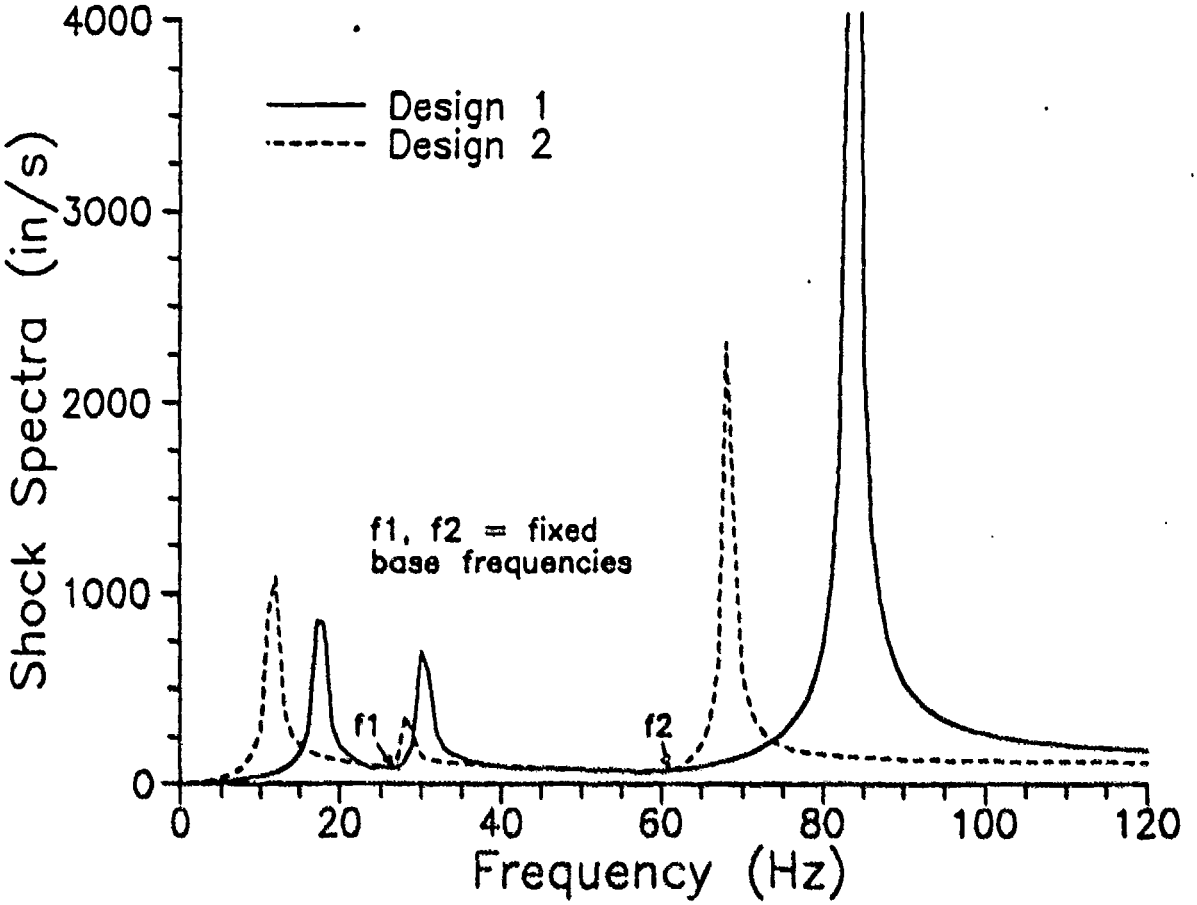

Fig. 8 - Shock response spectra for Designs 1 and 2.

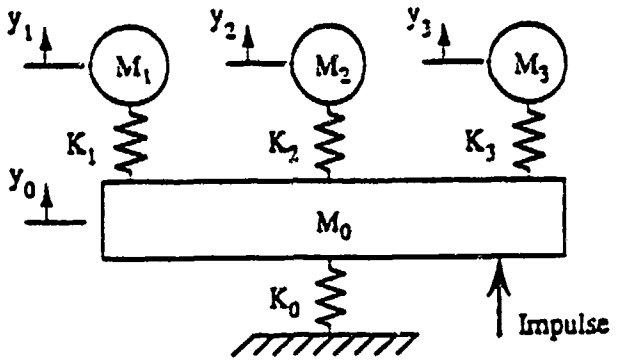

$\beta^2 = K_1/M_1$ $\quad x_1 = y_1 - y_0$

$\gamma^2 = K_2/M_2$ $\quad x_2 = y_2 - y_0$

$\delta^2 = K_3/M_3$ $\quad x_3 = y_3 - y_0$

$\phi^2 = K_0/M_0$

Fig. 9 - Three-degree of freedom equipment attached to the vehicle M_0, K_0.

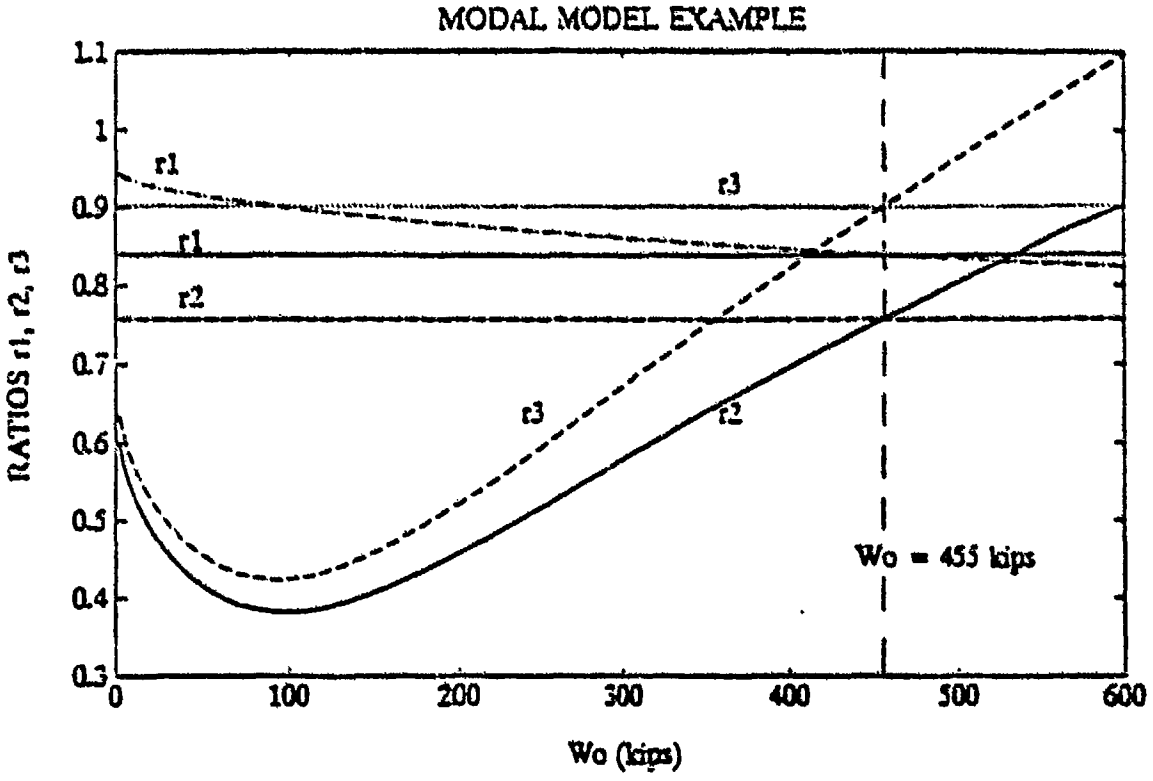

Fig. 10 - Shock design ratios versus the vehicle weight for $\phi = 0.9475\ \beta$.

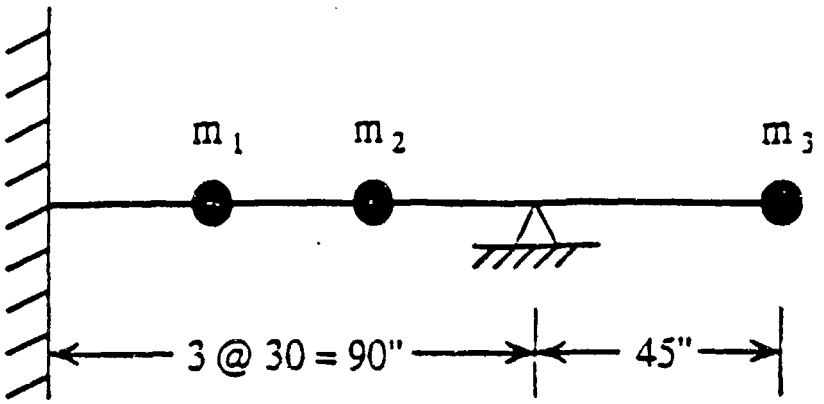

Fig. 11 - Example of an overhanging beam, $m_1 = m_2 = m_3$.

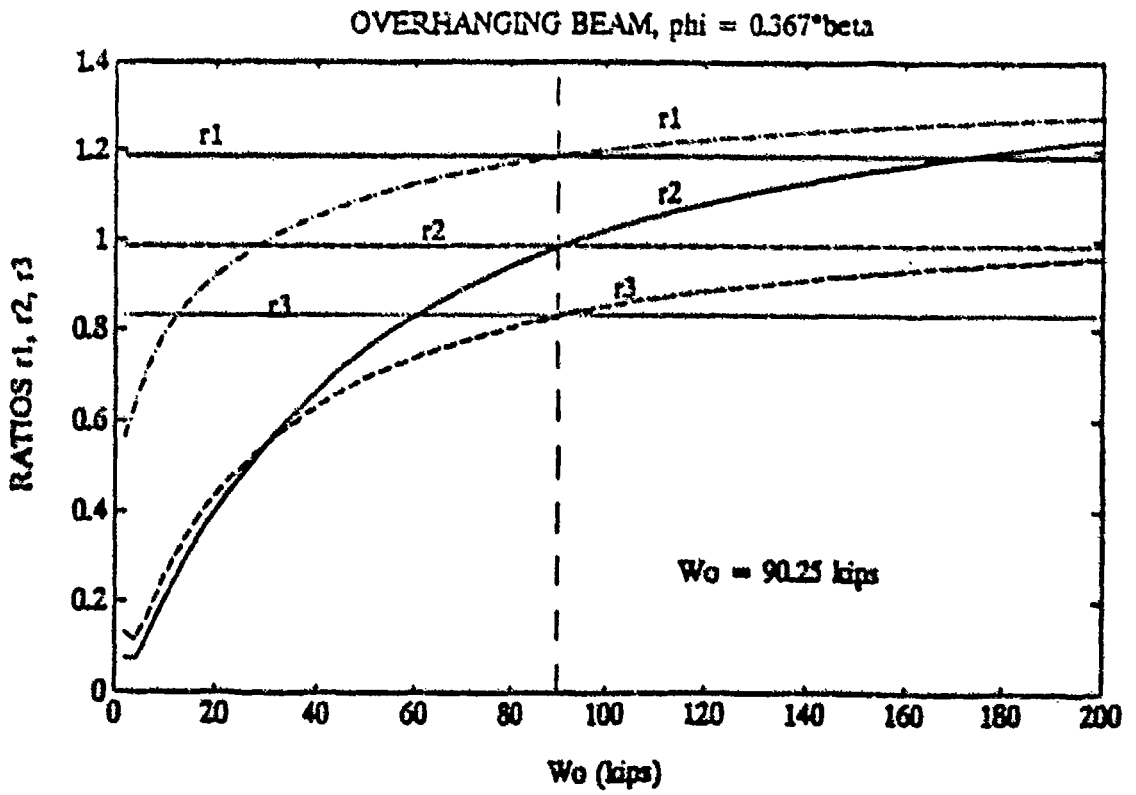

Fig. 12 - Shock design ratios versus the vehicle weight for $\phi = 0.367\ \beta$.

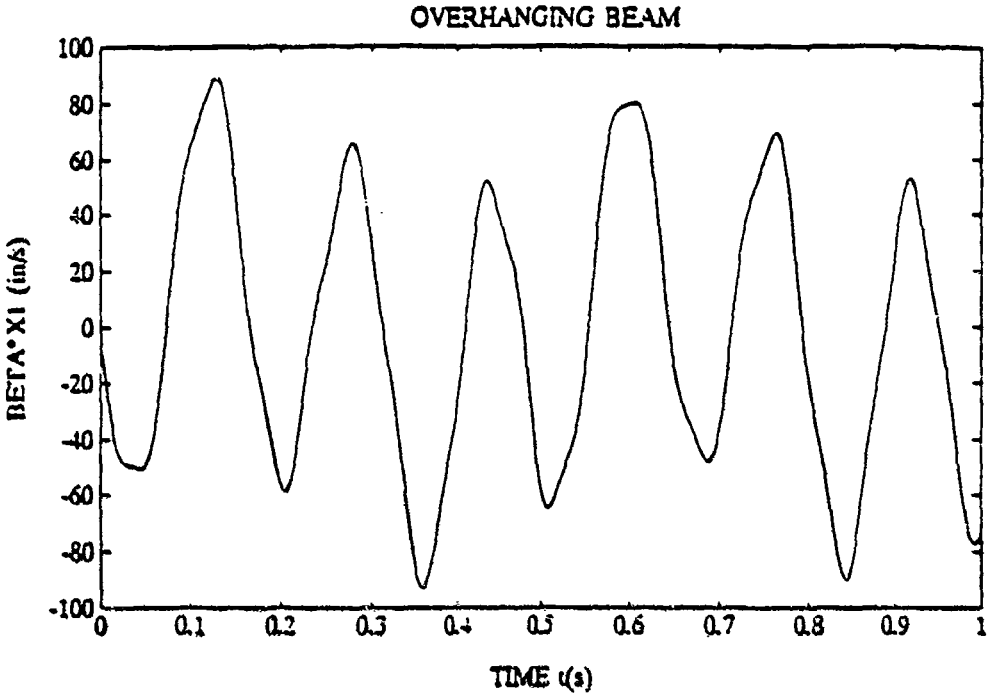

(a)

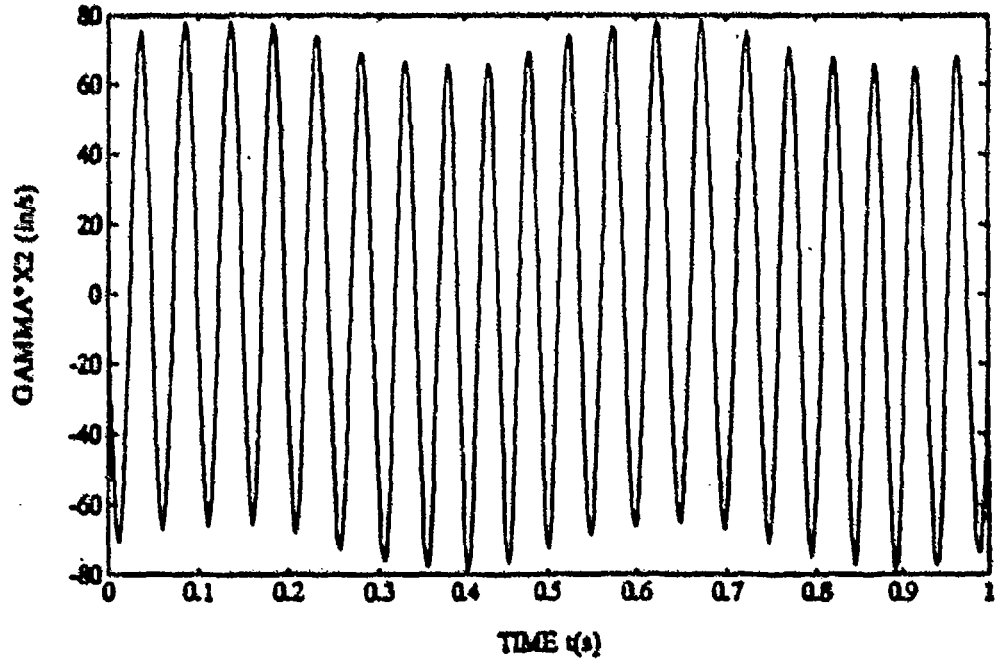

(b)

Fig. 13 - Time history motions for the overhanging beam; (a) βX_1, (b) γX_2, (c) δX_3.

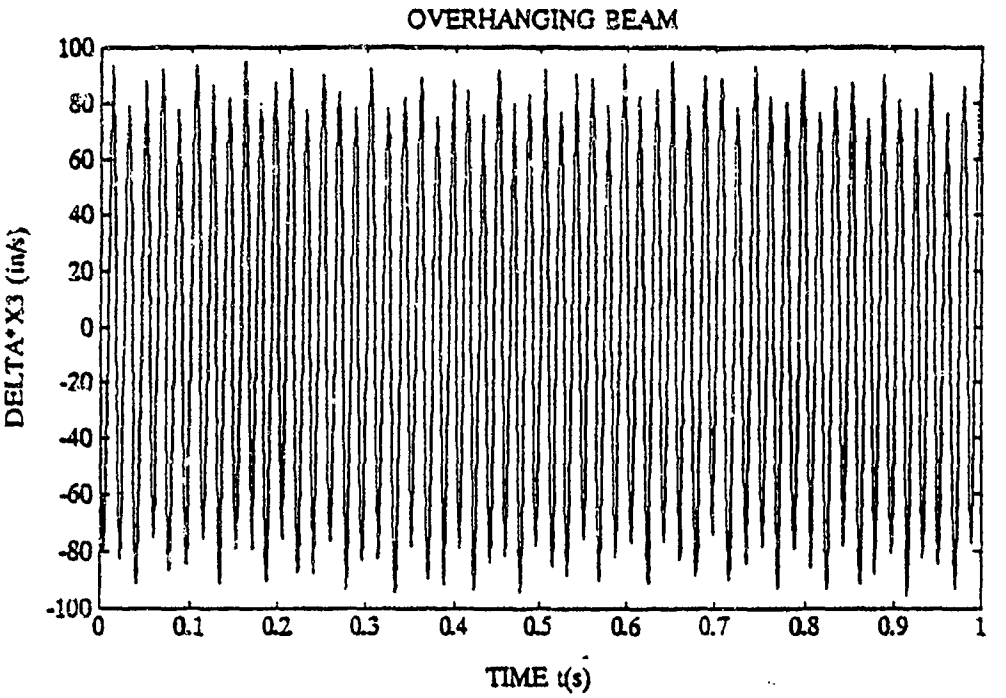
OVERHANGING BEAM
DELTA*X3 (in/s)
100
80
60
40
20
0
-20
-40
-60
-80
-100
0
0.1
0.2
0.3
0.4
0.5
0.6
0.7
0.8
0.9
1
TIME t(s)

(c)

Fig. 13

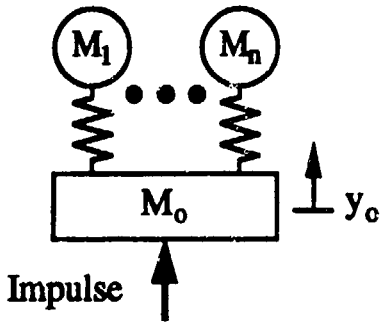

Vehicle 1

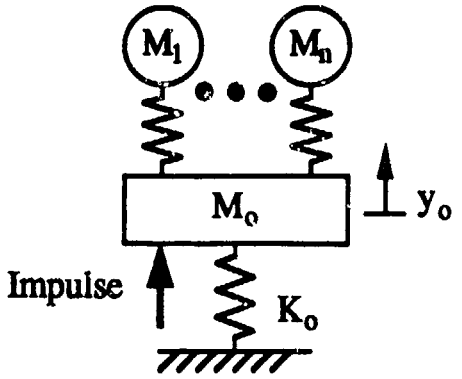

Vehicle 2

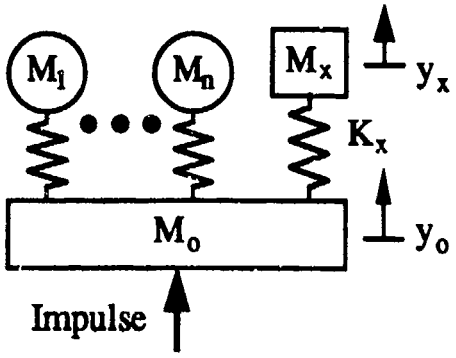

Vehicle 3

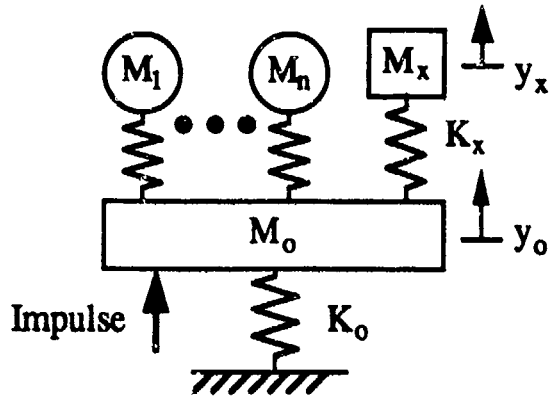

Vehicle 4

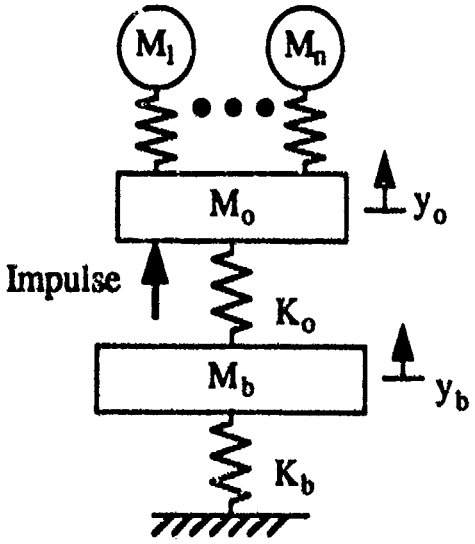

Vehicle 5

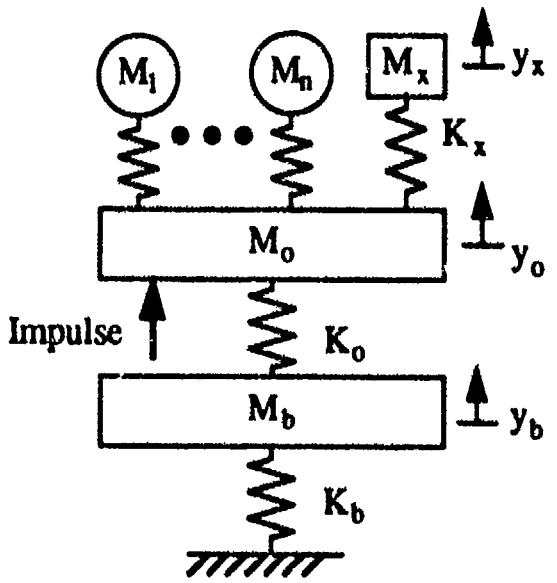

Vehicle 6

Fig. 14 - Vehicles used in the optimization modeling method.

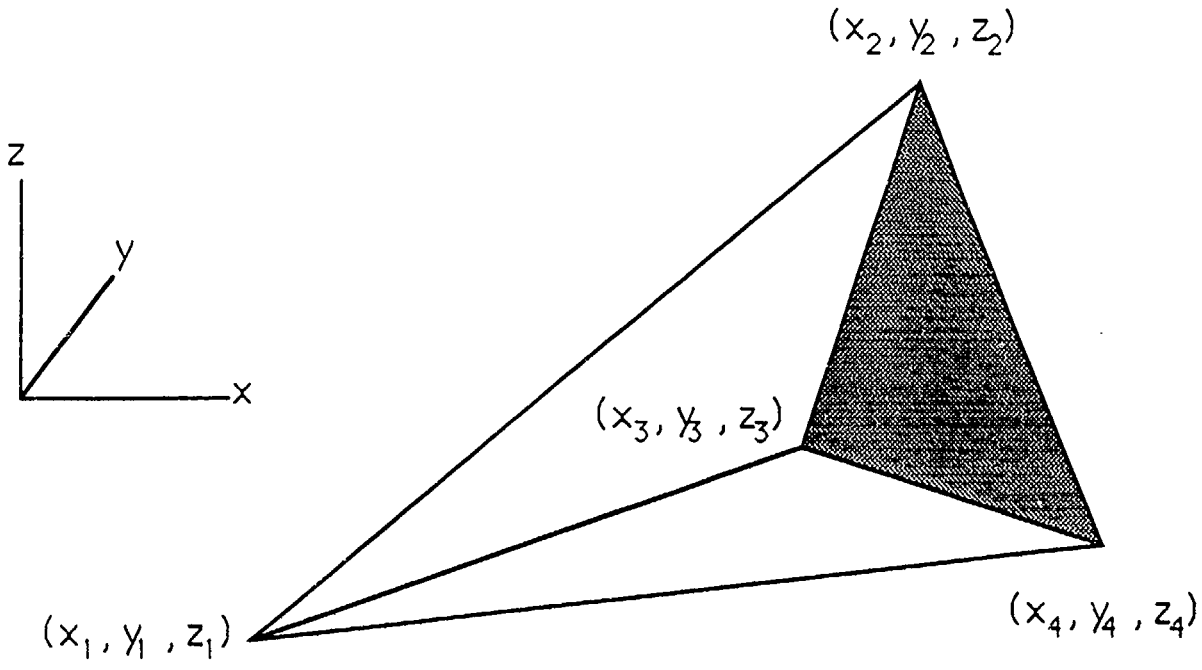

Fig. 15 - Simplex with 4 vertices is a tetrahedron.

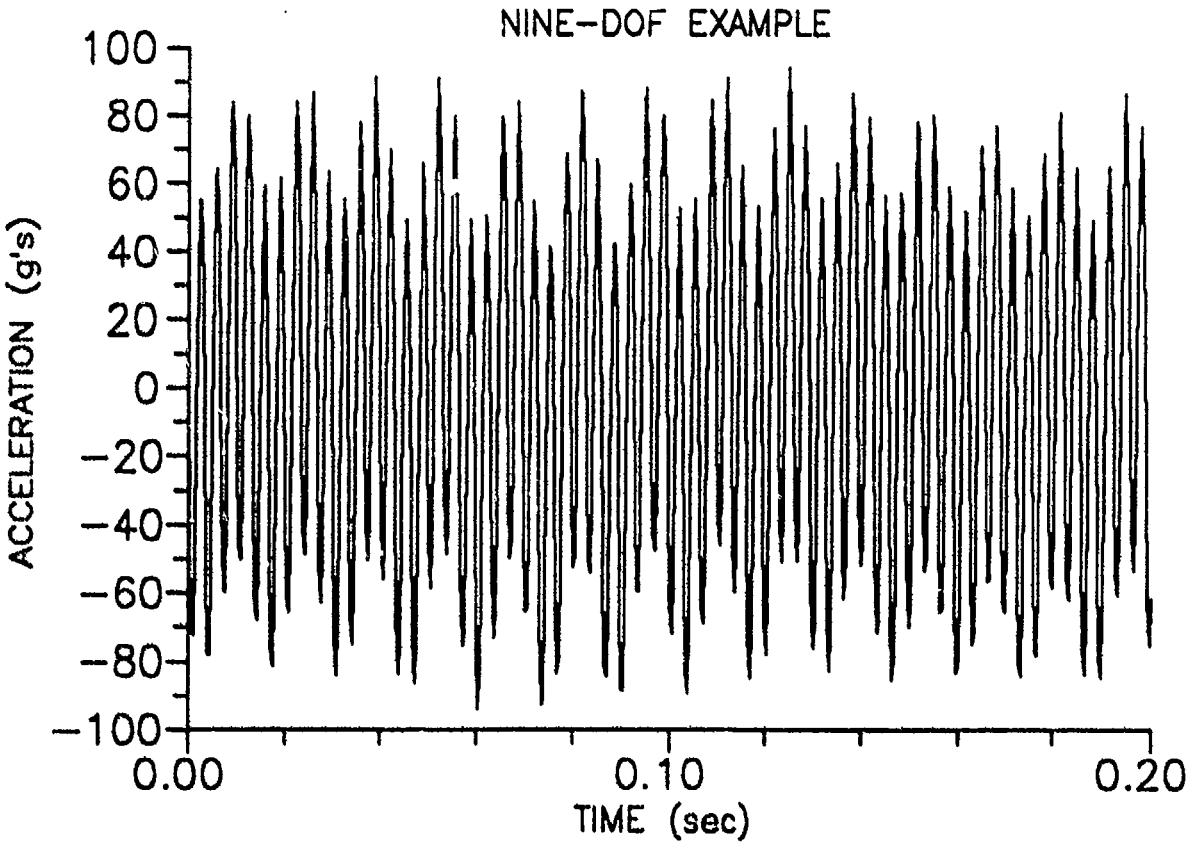

Fig. 16 - Sample of the Time-History Motion of Modal Mass 6.